Upon Intranasal Vesicular Stomatitis Virus Infection, Astrocytes in the Olfactory Bulb Are Important Interferon Beta Producers That Protect from Lethal Encephalitis

Claudia N. Detje,[a] Stefan Lienenklaus,[b] Chintan Chhatbar,[a] Julia Spanier,[a] Chittappen K. Prajeeth,[c] Claudia Soldner,[a] Michael G. Tovey,[d] Dirk Schlüter,[e,f] Siegfried Weiss,[b] Martin Stangel,[c] Ulrich Kalinke[a]

Institute for Experimental Infection Research, TWINCORE, Centre for Experimental and Clinical Infection Research, a joint venture between the Hannover Medical School and the Helmholtz Centre for Infection Research, Hannover, Germany[a]; Molecular Immunology, Helmholtz Centre for Infection Research, Braunschweig, Germany[b]; Clinical Neuroimmunology and Neurochemistry, Department of Neurology, Hannover Medical School, Hannover, Germany[c]; Laboratory of Biotechnology Applied Pharmacology, École Normale Supérieure de Cachan, Cachan Cedex, France[d]; Institute for Medical Microbiology and Hospital Hygiene, Otto-von-Guericke-University Magdeburg, Magdeburg, Germany[e]; Organ-Specific Immune Regulation, Helmholtz Centre for Infection Research, Braunschweig, Germany[f]

ABSTRACT Previously we found that following intranasal (i.n.) infection with neurotropic vesicular stomatitis virus (VSV) type I interferon receptor (IFNAR) triggering of neuroectodermal cells was critically required to constrain intracerebral virus spread. To address whether locally active IFN-β was induced proximally, we studied spatiotemporal conditions of VSV-mediated IFN-β induction. To this end, we performed infection studies with IFN-β reporter mice. One day after intravenous (i.v.) VSV infection, luciferase induction was detected in lymph nodes. Upon i.n. infection, luciferase induction was discovered at similar sites with delayed kinetics, whereas on days 3 and 4 postinfection enhanced luciferase expression additionally was detected in the foreheads of reporter mice. A detailed analysis of cell type-specific IFN-β reporter mice revealed that within the olfactory bulb IFN-β was expressed by neuroectodermal cells, primarily by astrocytes and to a lesser extent by neurons. Importantly, locally induced type I IFN triggered distal parts of the brain as indicated by the analysis of ISRE-eGFP mice which after i.n. VSV infection showed enhanced green fluorescent protein (eGFP) expression throughout the brain. Compared to wild-type mice, IFN-β$^{-/-}$ mice showed increased mortality to i.n. VSV infection, whereas upon i.v. infection no such differences were detected highlighting the biological significance of intracerebrally expressed IFN-β. In conclusion, upon i.n. VSV instillation, IFN-β responses mounted by astrocytes within the olfactory bulb critically contribute to the antiviral defense by stimulating distal IFN-β-negative brain areas and thus arresting virus spread.

IMPORTANCE The central nervous system has long been considered an immune privileged site. More recently, it became evident that specialized immune mechanisms are active within the brain to control pathogens. Previously, we showed that virus, which entered the brain via the olfactory route, was arrested within the olfactory bulb by a type I IFN-dependent mechanism. Since peripheral type I IFN would not readily cross the blood-brain barrier and within the brain thus far no abundant type I IFN responses have been detected, here we addressed from where locally active IFN originated from. We found that upon intranasal VSV instillation, primarily astrocytes, and to a lesser extent neurons, were stimulated within the olfactory bulb to mount IFN-β responses that also activated and protected distal brain areas. Our results are surprising because in other infection models astrocytes have not yet been identified as major type I IFN producers.

Viral infections of the central nervous system are comparably rare but potentially devastating conditions. Typically, neurotropic viruses may reach the central nervous system (CNS) by (i) the olfactory route, (ii) via the blood-brain barrier, (iii) by infecting infiltrating cells, or (iv) by axonal transport (1). Viral clearance in non-neuronal tissues often involves cytolytic elimination of infected cells. However, owed to their longevity and low regeneration potential this is not a suitable option for the clearance of neurotropic viruses from infected neurons. Nevertheless, many viral infections can be cleared from the CNS without causing marked neurological damage. Obviously, this is conferred by immune mechanisms that clear virus from infected tissues, or that inhibit viral replication, without affecting structure and function of the nervous system (2).

To analyze neuroinfection via the olfactory route, intranasal (i.n.) infection of mice with vesicular stomatitis virus (VSV) is broadly studied. VSV is a negative-strand RNA virus, which is distantly related to rabies virus. Unlike rabies virus, VSV is a highly cytopathic virus (3). Upon i.n. instillation, VSV infects olfactory sensory neurons in the nasal mucosa and moves along axons to the

glomerular layer of the olfactory bulb. There, virus spread is efficiently arrested by a type I interferon (IFN)-dependent mechanism ([4]). Activation of astrocytes and astrogliosis were observed as early as 1 day postinfection (p.i.) and peaked around day 8. Significant microgliosis was not observed before day 3 ([5]). Since type I IFN produced in the periphery does not readily cross the blood-brain barrier, it was speculated that upon i.n. VSV infection protective type I IFN was produced locally within the CNS. Although all nucleated cells are able to produce type I IFNs *in vitro*, plasmacytoid dendritic cells (pDCs) were shown to be important type I IFN producers in several viral infections ([6], [7]). However, pDCs were reported to be absent from brain ([8]). This raised the question which CNS cell subset would produce protective type I IFN upon i.n. VSV infection.

Previous studies showed that upon influenza and La Crosse virus infection, type I IFN was conveyed by parenchymal cells of the CNS such as microglia/macrophages, ependymal cells and neurons ([9], [10]). Of note, all cells of the CNS are able to react to IFN stimulation ([11]), although it is unclear how assessable cells in different areas of the CNS are for soluble factors such as cytokines. One recent report suggested that locally produced type I IFN might act as a long-distance effector ([12]).

Notably, among type I IFNs, IFN-α may exhibit toxic effects within the CNS as demonstrated by transgenic mice with brain-specific overexpression of IFN-α. Such mice displayed progressive encephalopathy that resembled the Aicardi-Goutièrez syndrome in humans ([13]). Several studies implied that under steady-state conditions or during infectious disease, primarily IFN-β but not IFN-α was induced within the CNS ([14]). Consequently, we here addressed whether upon i.n. VSV infection IFN-β and IFN-α were induced locally within the CNS and which subset of cells expressed IFN-β. Our results indicate that protective IFN-β was primarily produced within the olfactory bulb by astrocytes and that this IFN exerted its protective effects throughout the brain. Most importantly, mice with an IFN-β deletion showed enhanced sensitivity to i.n. VSV infection, further highlighting the nonredundant role of intracerebral IFN-β in antiviral protection.

MATERIALS AND METHODS

Mice. IFN-β$^{-/-}$ ([15]), IFN-β$^{\Delta\beta\text{-luc/wt}}$ ([16]), and ISRE-eGFP ([17]) mice were backcrossed to the C57BL/6JOlaHsd background before intercrossing with other transgenic mouse strains. IFN-β$^{\Delta\beta\text{luc/wt}}$ mice used for *in vivo* imaging were backcrossed to C57BL/6 albino background ([18]). Tissue-specific reporter mice were generated by intercrossing IFN-β$^{\text{floxβ-luc/floxβ-luc}}$ animals with transgenic mice that express Cre tissue-specifically. To selectively enable the reporter system in neuroectodermal cells, neurons, astrocytes, or oligodendrocytes, Nes-Cre$^{+/-}$ ([19]), Syn1Cre$^{+/-}$ ([20]), GFAPCre$^{+/-}$ ([21]), or MOGiCre$^{+/-}$ ([22]) mice were used, respectively. Mice were kept under specific-pathogen-free conditions in the central mouse facility of the TWINCORE and at the Helmholtz Centre for Infection Research. Unmutated congenic C57BL/6JOlaHsd mice, also referred to as wild-type (WT) mice, were purchased at Harlan-Winkelmann. Animal experiments were conducted in compliance with German federal and state legislation on animal experiments.

Viruses. VSV-Indiana (Mudd-Summers isolate), originally obtained from D. Kolakofsky (University of Geneva, Switzerland), was grown on BHK-21 cells. Virus was harvested from cell culture supernatants, and titers were determined by plaque formation on Vero cells.

Intranasal VSV infection and optical imaging. For i.n. infection, a total of 10 µl of suspension containing VSV in phosphate-buffered saline (PBS) was pipetted into both nostrils of anesthetized mice. For fluorescence imaging mice were sacrificed and brains were analyzed in a CRI

Maestro2 imaging system (INTAS). For *in vivo* imaging, luciferase reporter mice were intravenously injected with 150 mg/kg of D-luciferin in PBS (Perkin-Elmer), anesthetized with 2.5% Isofluran (Abbot), and monitored using an IVIS Spectrum CT (Perkin-Elmer). Photon flux was quantified using the Living Image 4.3.1 software. For *ex vivo* luciferase activity measurements from selected tissues, mice were transcardially perfused with PBS prior to sacrificing them. Then, the weight of tissue fragments was determined, and fragments were homogenized in reporter lysis buffer (Promega) using a FastPrep24 homogenator. Lysates were mixed with a BrightGlo luciferase assay system (Promega), and luminescence was detected using a Centro XS^3 plate reader (Barthold).

Astrocyte isolation and stimulation. Astrocytes were purified from neonatal mice as described previously ([23]). For stimulation experiments, astrocytes were plated at a density of 10^5 cells/ml in 12-well plates. After 24 h of cultivation, the medium was changed, and cells were stimulated with either poly(I·C) or VSV. After 18 h of incubation, cell-free supernatant was harvested and stored at −20°C.

Real-time PCR. For the analysis of interferon mRNA expression, mice were transcardially perfused with PBS, and brains were isolated and lysed in TRIzol (Life Technologies). RNA was isolated and purified with an RNeasy Mini Kit (Qiagen), and cDNA was synthesized using a QuantiTect reverse transcription kit (Qiagen). To analyze IFN mRNA expression, an IFN-subtype-specific dual-probe TaqMan-PCR assay (QuantiFast probe assay [Qiagen]) with the housekeeper gene *ppia2* as a control was performed. All kits were used according to the manufacturer's protocol.

ELISA. To determine the IFN content of serum or cell culture supernatant, a mouse VeriKine IFN-β enzyme-linked immunosorbent assay (ELISA) kit (PBL), a mouse VeriKine-HS IFN-β ELISA kit (PBL), or a VeriKine mouse IFN-α ELISA kit (PBL) was used according to the manufacturer's protocols.

Statistical analysis. Data were analyzed using R (R Core Team 2014) deploying Dunnett-type simultaneous multiple contrast tests using functionalities provided by add-on package Multcomp ([24]) or GraphPad Prism 5.0 software.

RESULTS

In a previous study we observed normal pathogen control in IFN-β$^{-/-}$ mice infected intravenously (i.v.) with VSV ([6]). Here we revisited the role of IFN-β upon i.n. VSV infection. In confirmation, 12 and 24 h after i.v. infection with 2×10^6 PFU of VSV, wild-type (WT) control mice, as well as IFN-β$^{-/-}$ mice, showed maximal IFN-α serum levels, which declined at later time points and reached background levels by day 2 ([Fig. 1A], upper panel). Interestingly, IFN-β was not detected in the sera of i.v.-infected WT mice at any time point tested, whereas i.v. injection with poly(I·C) induced short-lived serum IFN-β peaking ~6 h after the treatment ([Fig. 1B], upper panel). Two days after i.n. infection with 10^3 PFU of VSV, maximal IFN-α levels were detected in the sera of WT and IFN-β$^{-/-}$ mice that declined within the following 2 days to background levels ([Fig. 1A], lower panel). Upon i.n. infection of WT mice, again no serum IFN-β was detected, whereas i.n. poly(I·C) treatment did induce detectable IFN-β responses ([Fig. 1B], lower panel). These data showed that upon i.v. and i.n. VSV infection, high levels of IFN-α, but not IFN-β, were detected in the serum. Both WT and IFN-β$^{-/-}$ mice mounted IFN-α responses of similar magnitudes.

To address whether VSV infection induces local IFN-β responses that could not be detected in the serum by the available ELISA methods, we studied IFN-β reporter mice carrying one IFN-β allele in which the IFN-β was replaced by luciferase (IFN-β$^{\Delta\beta\text{luc/wt}}$). It has been reported previously that in these mice luciferase expression is equivalent to IFN-β expression, and can be used as a direct measure of IFN-β expression ([16]). We observed
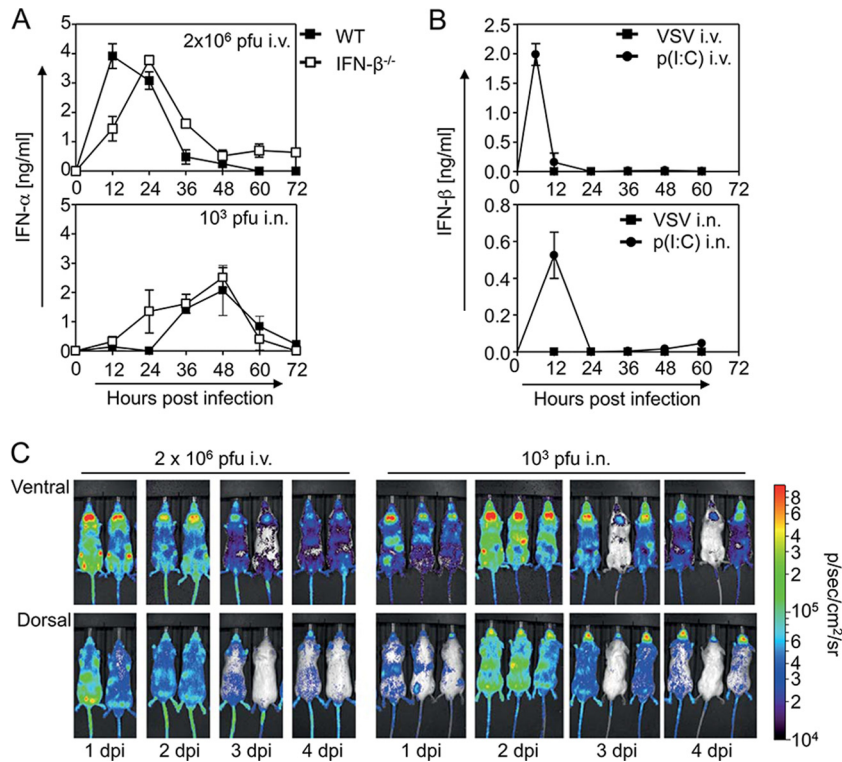
FIG 1 Upon i.n. VSV instillation, IFN-α but not IFN-β is detectable in serum, whereas IFN-β is induced within the CNS. (A) C57BL/6 WT ($n = 5$) and IFN-β$^{-/-}$ mice ($n = 5$) were i.v. or i.n. infected with 2×10^6 or 10^3 PFU of VSV, respectively. At the indicated time points, blood samples were drawn. After centrifugation of blood samples, serum was taken and IFN-α levels were determined by an ELISA method. The results of one of two independent experiments are shown. (B) C57BL/6 WT mice ($n = 5$) were either i.v. or i.n. infected with 2×10^6 or 10^3 PFU of VSV, respectively. Blood samples were drawn at the indicated time points, and serum IFN-β levels were determined by an ELISA method. As a positive control, WT mice were treated i.n. or i.v. with 10 μg of poly(I·C), and the serum IFN-β levels were determined. The results of one of two independent experiments are shown. (C) IFN-β luciferase reporter mice (IFN-β$^{\Delta\beta\text{-luc/wt}}$) were i.v. or i.n. infected with 2×10^6 and 10^3 PFU of VSV, respectively. For analysis of luciferase expression, luciferin was i.v. injected 1, 2, 3, or 4 days p.i., and mice were monitored in an IVIS Spectrum CT *in vivo* imager.

similar survival of IFN-β$^{\Delta\beta\text{luc/wt}}$ and WT mice upon i.n. and i.v. VSV infection, respectively, indicating that the deletion of one IFN-β allele had no significant impact on the virus control (data not shown). One day after i.v. infection of IFN-β$^{\Delta\beta\text{luc/wt}}$ with 2×10^6 PFU of VSV, strong luciferase induction was observed in secondary lymphoid organs and particularly in the inguinal and cervical lymph nodes (Fig. 1C, left panels). Upon i.n. challenge with 10^3 PFU of VSV, the strongest luciferase induction was detected 2 days p.i. (Fig. 1C, right panels). Similar to the results obtained with i.v.-infected mice, i.n. infection induced the strongest luciferase induction in cervical lymph nodes (Fig. 1C, upper right panels). Interestingly, in the dorsal view of i.n. infected mice luciferase signals were also detected in the forehead region which reached maximal strength between days 3 and 4 p.i. (Fig. 1C, lower right panels, and Fig. 2A).

To address whether luciferase signals detected in the forehead of i.n.-infected IFN-β reporter mice originated from cells within the CNS, IFN-β reporter mice were i.n. infected with 10^3 PFU of VSV; on day 4 the mice were sacrificed, and homogenates of different brain areas were analyzed for luciferase activity separately. Interestingly, high luciferase activity was only detected in the olfactory bulb, whereas in the cerebrum, cerebellum, and brain stem luciferase activity was ~1,000-fold lower (Fig. 2B).

To identify the cell type showing IFN-β induction within the olfactory bulb, conditional IFN-β reporter mice (IFN-β$^{\text{floxβ-luc/wt}}$)

were intercrossed with transgenic mice expressing Cre only in neuroectodermal cells (NesCre$^{+/-}$), neurons of the CNS (Syn1Cre$^{+/-}$), astrocytes (GFAPCre$^{+/-}$), or oligodendrocytes (MOGiCre$^{+/-}$). Interestingly, NesCre$^{+/-}$IFN-β$^{\text{floxβ-luc/wt}}$ mice showed similar, but still moderately reduced, luciferase activity within the olfactory bulb compared to IFN-β$^{\Delta\beta\text{luc/wt}}$ mice at 3 days p.i. (Fig. 2C). These results indicated that ca. 87% of the luciferase signal detected in IFN-β$^{\Delta\beta\text{-luc/wt}}$ mice had a neuroectodermal origin (Fig. 2D). Notably, Syn1Cre$^{+/-}$ IFN-β$^{\text{floxβ-luc/wt}}$ mice showed low and GFAPCre$^{+/-}$ IFN-β$^{\text{floxβ-luc/wt}}$ mice showed enhanced luciferase activities, the latter of which was still reduced compared to that detected in IFN-β$^{\Delta\beta\text{-luc/wt}}$ or NesCre$^{+/-}$ IFN-β$^{\text{floxβ-luc/wt}}$ mice (Fig. 2C). These data implied that upon i.n. VSV infection, astrocytes and to a lesser extent neurons expressed IFN-β.

To confirm in an independent system that upon VSV treatment astrocytes can mount IFN-β responses, we enriched astrocytes from neonatal mixed glia cell cultures and infected them with VSV or stimulated them with the strong IFN inducer poly(I·C). After 18 h of incubation, cell-free supernatant was collected, and the interferon content was determined by ELISA methods. Upon VSV infection, enhanced IFN-β was detected (Fig. 2E) that was still low compared to IFN-β responses induced by poly(I·C) (Fig. 2F). Importantly, neither upon VSV nor poly(I·C) stimulation astrocytes produced IFN-α2 or -α4 (data not shown).
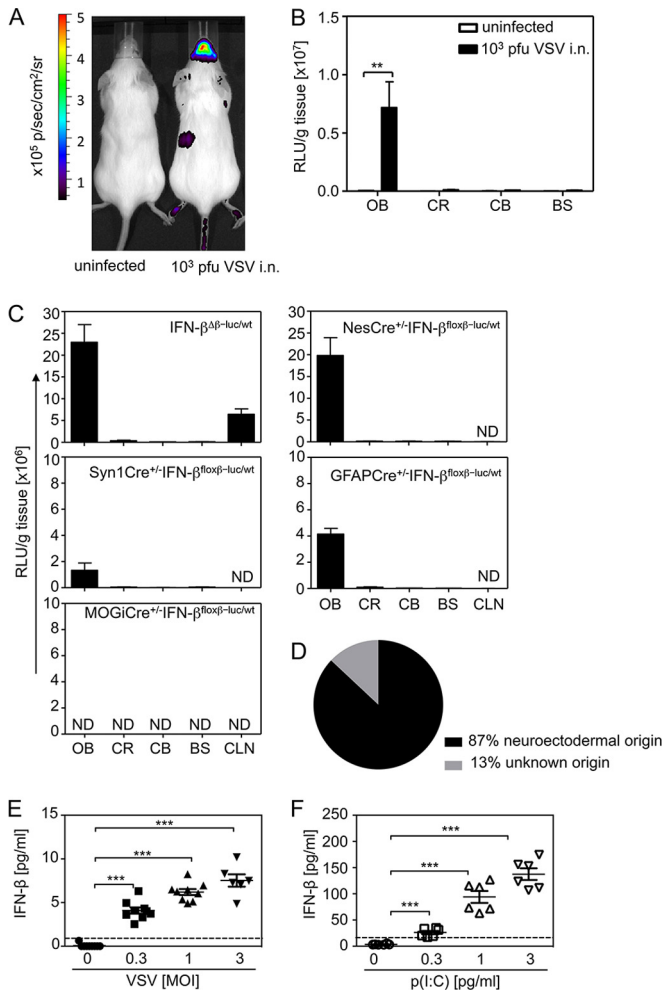
FIG 2 Upon i.n. VSV infection, primarily neuroectodermal cells in the olfactory bulb express IFN-β. (A and B) IFN-β luciferase reporter mice (IFN-β$^{\Delta\beta-luc/wt}$) were i.n. infected with 10^3 PFU of VSV. On day 3 p.i., one mouse was exemplarily imaged in an *in vivo* imager, whereas the other mice were perfused with PBS to obtain blood-free tissues and sacrificed. The brains were dissected in olfactory bulbs, cerebra, cerebella, and brain stems, the tissues were lysed, and the luciferase activity was determined. (C) To study the identity of neuroectodermal cells, i.e., astrocytes, neurons, or oligodendrocytes, that were the main IFN-β producers within the CNS, tissue-specific reporter mice were used. These mice were i.n. infected with 10^3 PFU of VSV. At 4 days p.i., mice were perfused and sacrificed, and olfactory bulbs (OB), cerebra (CR), cerebella (CB), brain stems (BS), and cervical lymph nodes (CLN) were prepared. Tissues were lysed, and the luciferase activity was determined. The data from one representative experiment out of two to five independent ones are shown. For each data set, at least five mice per group were used. (D) Estimation of the luciferase signal obtained in the olfactory bulb of i.n.-infected NesCre$^{+/-}$IFN-β$^{flox\beta-luc/wt}$ relative to IFN-β$^{\Delta b-luc/wt}$ mice. Astrocytes were isolated from mixed glial cultures of WT mice and treated with VSV at the indicated multiplicity of infection (MOI) (E) or with poly(I·C) (F) at the indicated final concentrations. After 18 h of incubation, cell-free supernatant was collected, and the IFN-β content was determined by ELISA methods. The combined data of three independent experiments are shown (***, $P < 0.0001$ [Dunnett-type multiple comparison procedure]).

Collectively, these experiments indicated that after i.n. VSV infection among neuroectodermal cells astrocytes and, to a lesser extent neurons, showed enhanced IFN-β expression, whereas oligodendrocytes did not contribute to IFN-β responses within the

CNS. Nevertheless, it cannot be excluded that non-neuroectodermal cells of the CNS such as microglia also produced some IFN-β.

Reverse transcription-PCR (RT-PCR) analysis of IFN-β and 10 different IFN-α subtypes revealed that, within 2 days after i.n. VSV instillation, primarily IFN-β was induced within CNS (Fig. 3A). Interestingly, constitutive low-level IFN-α2 expression was increased within 2 days after infection, whereas IFN-α4 and IFN-α5 were only moderately induced at this time point. Induction of other IFN-α subtypes was not detected (Fig. 3A). Extended analysis of IFN-β, IFN-α2, IFN-α4, and IFN-α5 expression in different brain areas showed that the majority of IFN transcripts were found within the olfactory bulb (Fig. 3B). These results were in line with the observation that in i.n.-infected reporter mice, luciferase induction was primarily detected within the olfactory bulb (compare Fig. 1C, Fig. 2B, and Fig. 3B).

To address whether IFN-β that was locally induced within the olfactory bulb was only locally active or also showed long-distance effects, we performed experiments with ISRE-eGFP mice. In such mice type I IFN-stimulated cells display enhanced green fluorescent protein (eGFP) expression (17). One, two, and three days after i.n. infection with 10^3 PFU of VSV, mice were sacrificed, and the brains were prepared and studied in a fluorescence imager. Already, at 1 day after i.n. infection, whole brains of ISRE-eGFP mice showed enhanced eGFP expression that further increased with time (Fig. 3C, left panels, and Fig. 3D, upper panel). Of note, enhanced eGFP expression was not confined to the site of local IFN-β induction, i.e., the olfactory bulb, but was also found in distal brain areas. Importantly, ISRE-eGFP mice devoid of IFN-β (ISRE-eGFP$^{+/-}$ IFN-β$^{-/-}$) did not show enhanced eGFP expression upon i.n. VSV challenge (Fig. 3C, right panels, and Fig. 3D, lower panel).

The data obtained thus far suggested that IFN-β played an important role within the CNS to constrain virus spread, whereas VSV infection did not appear to trigger abundant IFN-β serum levels. To address the role of IFN-β in peripheral infection compared to neuroinfection, we performed a thorough dose sensitivity infection study of WT and IFN-β$^{-/-}$ mice. WT controls and IFN-β-deficient mice showed a very similar sensitivity to i.v. infection with 2×10^6, 2×10^7, 2×10^8, and 2×10^9 PFU of VSV (Fig. 4A and B). Importantly, IFN-β$^{-/-}$ mice were significantly more vulnerable to i.n. VSV infection than WT controls, as indicated by 80% of WT mice surviving i.n. instillation of 10^3 PFU of VSV, whereas under such conditions all IFN-β$^{-/-}$ mice died (Fig. 4C and D). Along the same line, for several days following i.v. infection with 2×10^6 PFU of VSV, no virus could be detected in the olfactory bulbs, cerebra, cerebella, and brain stems of WT mice (Fig. 4E, upper panel). Similarly, also in IFN-β$^{-/-}$ mice hardly any virus was found (Fig. 4E, lower panel). However, upon i.n. infection with 10^3 PFU of VSV, the brains of IFN-β$^{-/-}$ mice displayed significant virus burden that further increased over time (Fig. 4F, lower panel), whereas WT animals were virus free (Fig. 4F, upper panel).

DISCUSSION

Here we showed that, upon i.n. VSV infection, antiviral IFN-β was induced locally within the olfactory bulb by astrocytes and, to a lesser extent, by neurons. Although produced locally, IFN-β exhibited long-distance effects on distal brain areas. In addition, IFN-β-deficient mice displayed enhanced sensitivity to i.n. VSV
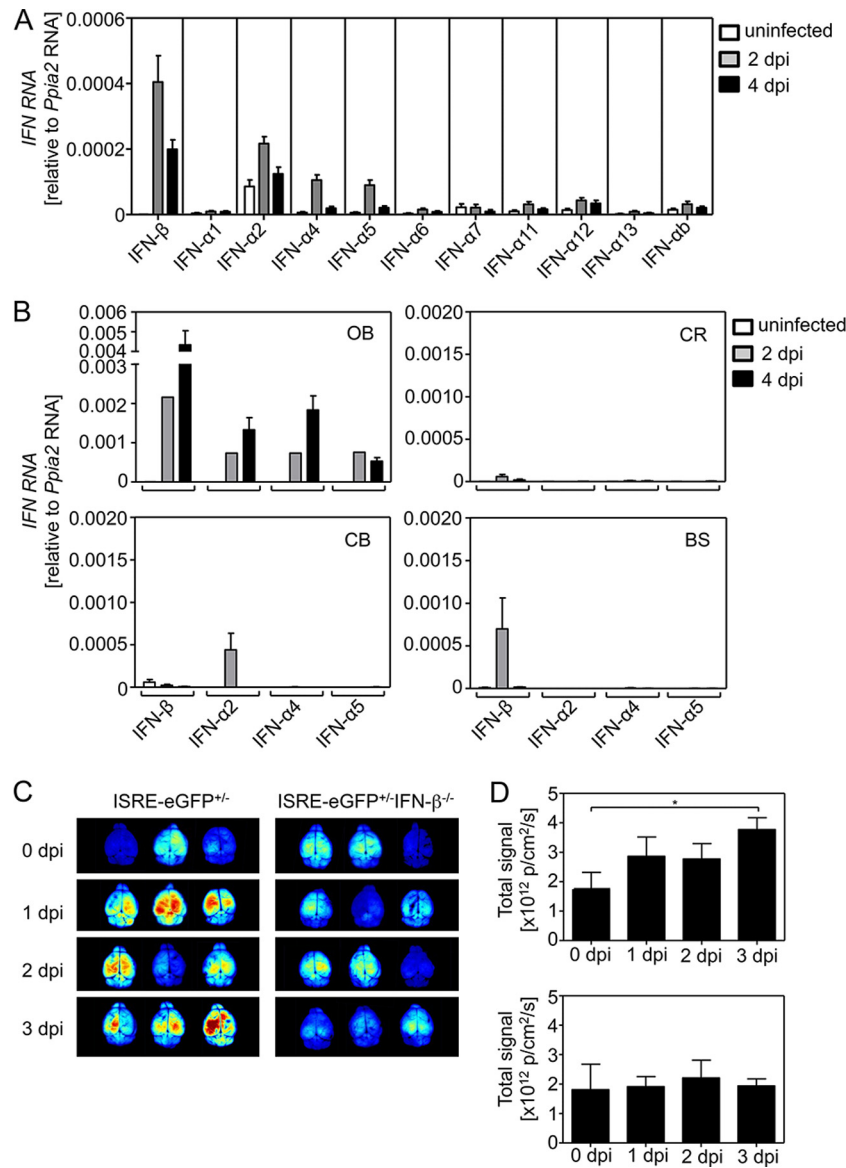
FIG 3 IFN-β induced locally within the olfactory bulb also stimulates distal parts of the CNS. (A) Mice were i.n. infected with 10^3 PFU of VSV. At 2 and 4 days p.i. the mice were perfused, and the brains were prepared and lysed in TRIzol. RNA was isolated, purified, and used for cDNA synthesis. To analyze IFN mRNA expression, IFN-subtype-specific TaqMan PCRs were performed. (B) Mice were treated as described above. After perfusion, the brains were prepared and dissected into olfactory bulbs (OB), cerebra (CR), cerebella (CB), and brain stems (BS). Brain regions were lysed in TRIzol, and RNA was isolated. After a purification step, cDNA synthesis and TaqMan PCR were performed for IFN-β, IFN-α2, IFN-α4, and IFN-α5. (C) ISRE-eGFP$^{+/-}$ and ISRE-eGFP$^{+/-}$ IFN-β$^{-/-}$ reporter mice were i.n. infected with 10^3 PFU of VSV. At the indicated time points, mice were sacrificed, and the eGFP expression was analyzed in a CRI Maestro 2 fluorescence imager (Intas). Representative samples of three independent experiments (15 mice per group in total) are shown. A spectral unmixing algorithm was used to subtract background autofluorescence. (D) The total signal of the brains was evaluated by definition of equal circular regions of interest over the entire brain using the provided software (*, $P \leq 0.05$ [Mann-Whitney test]).

infection, illustrating the biological significance of intracerebrally produced IFN-β.

In many cell types, the immediate-early type I IFN response is dominated by IFN-β (25). Therefore, it was speculated that IFN-β has a central regulatory function in priming cells for the induction of IFN-α genes (26, 27). Here we showed that upon i.v. VSV infection IFN-α responses of IFN-β$^{-/-}$ mice were only moderately delayed compared to WT mice, and overall resistance to VSV infection was not affected. Interestingly, under such conditions no serum IFN-β responses were detected. Correspondingly, i.n. VSV infection induced similar IFN-α serum responses in WT and IFN-

β$^{-/-}$ mice. This is in line with previous findings that upon infection with VSV, Sindbis virus, or Friend virus, IFN-α induction was independent of IFN-β (6, 28, 29).

Our *in vivo* imaging studies indicated that upon i.n. VSV instillation IFN-β was induced in the area of the foreheads of C57BL/6 reporter mice. Isolation of brains from such reporter mice and determination of luciferase activity within the different brain areas unequivocally revealed that IFN-β induction was only detected in the olfactory bulb but not in other brain areas. This observation was further confirmed by an independent method, i.e., by qPCR analysis of type I IFN mRNA induction. Of note, in
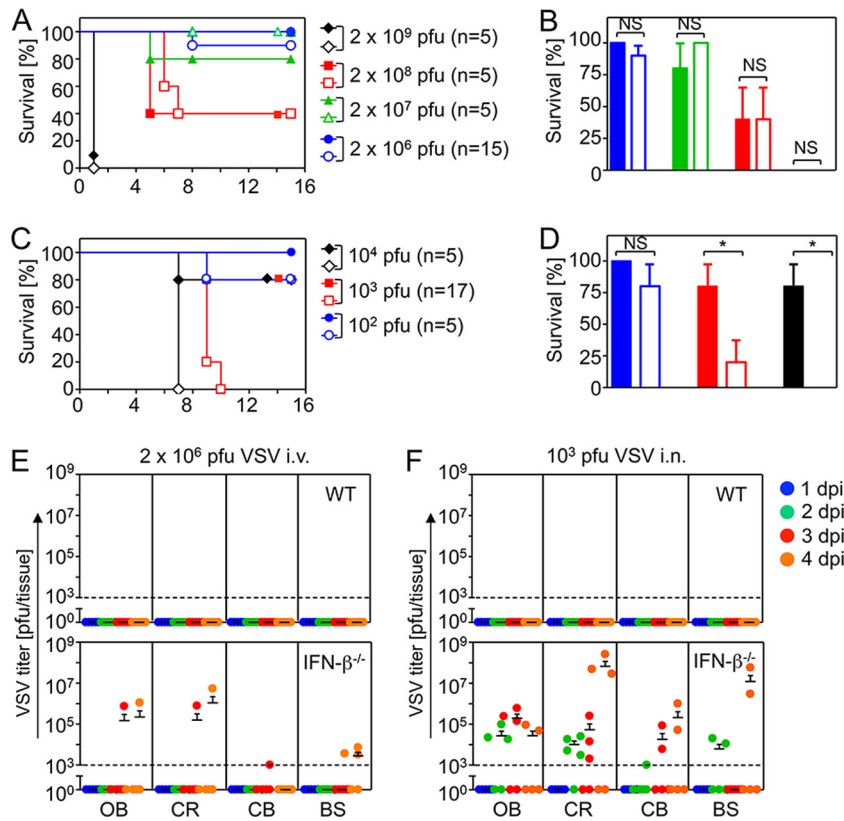
FIG 4 Upon i.n., but not i.v., challenge IFN-β-deficient mice show enhanced susceptibility to lethal VSV infection. (A) IFN-β$^{-/-}$ (open symbols) and C57BL/6 control mice (filled symbols) were i.v. infected with VSV at the indicated dosages, and survival was monitored. (B) No significant difference in the survival of infected WT and IFN-β$^{-/-}$ mice was observed at day 15 p.i. (C) Mice were i.n. infected with VSV at the indicated dosages, and survival was monitored. (D) At 15 days p.i., IFN-β$^{-/-}$ mice showed enhanced susceptibility to i.n. VSV infection when >10^3 PFU of VSV were applied. (E and F) To determine virus titers upon VSV infection, WT and IFN-β$^{-/-}$ mice were i.v. infected with 2 × 10^6 PFU (E) or i.n. infected with 10^3 PFU (F) of VSV. At 1, 2, 4, and 8 days p.i., the mice were sacrificed, and the virus titers in the olfactory bulbs (OB), cerebra (CR), cerebella (CB), and brain stems (BS) were determined based on plaque formation. Five mice per genotype and time point were analyzed.

an earlier study using BALB/c mice that were i.n. infected with VSV, no IFN-β induction was detected within the brain (30). Nevertheless, others have also recently detected IFN-β induction within the olfactory bulb upon i.n. VSV infection of C57BL/6 mice (12). Despite local IFN-β induction, in the present study we could not reisolate live virus from the olfactory bulbs of i.n.-infected C57BL/6 mice (Fig. 4F).

The analysis of tissue-specific reporter mice indicated that primarily astrocytes, and to a lesser extent neurons, showed IFN-β expression upon i.n. VSV infection. Our calculations implied that ca. 90% of locally induced IFN-β was expressed by neuroectodermal cells. However, since it is difficult to prove that NesCre$^{+/-}$ mice show Cre expression in 100% of all neuroectodermal cells, it cannot be excluded that the percentage underestimates the role of neuroectodermal cells in mounting type I IFN responses within the CNS. Furthermore, it is still possible that non-neuroectodermal cells such as microglia contributed as well, although such a contribution would certainly be a minor one. The luciferase expression detected in astrocyte-specific reporter mice and neuron-specific reporter mice did not add up to the quantity of luciferase activity detected in neuroectodermal reporter mice. This presumably can be explained by the fact that GFAPCre$^{+/-}$ mice express Cre only in a subset of astrocytes, notably activated astrocytes (21, 31). Similarly, although Synapsin-1 is expressed in neurons of the

olfactory bulb (32) and the deletion of Syn1Cre mice is highly selective, it is not very efficient. This might also result in a minor underestimation of the contribution of neurons to the overall IFN-β responses within the brain.

To address in an independent experimental setting whether upon VSV treatment astrocytes can mount IFN-β responses, we isolated astrocytes from mixed glial cultures and stimulated them with VSV or poly(I·C). Upon VSV infection, as well as poly(I·C) stimulation, IFN-β expression was significantly induced. Notably, astrocyte cultures stimulated with VSV showed enhanced IFN-β levels, although the absolute values were low compared to poly(I·C) stimulations. Importantly, VSV- or poly(I·C)-treated astrocytes did not produce IFN-α. Thus, considering the above *in vivo* experiments with astrocyte-specific GFAPCre$^{+/-}$ IFN-β$^{floxβ-luc/wt}$ reporter mice and the *in vitro* stimulation experiments with primary astrocytes, two independent lines of evidence supported the conclusion that upon VSV stimulation astrocytes are triggered to mount IFN-β responses.

Despite the fact that IFN-β was only locally induced within the olfactory bulb, we found long-distance IFNAR-signaling in distal brain parts such as the cerebrum and other brain areas. This observation was surprising because in our previous study we detected STAT1 phosphorylation as a measure of IFNAR signaling only within the glomerular layer of the olfactory bulb (4). This

discrepancy might be explained by the different readout systems. In our earlier study we analyzed IFNAR-triggered P-STAT-1 formation that is relatively short-lived and therefore can be easily missed. On the contrary, IFNAR-dependent eGFP-induction in ISRE-eGFP mice is a more robust readout simply due to the longevity of eGFP, which in previous studies was estimated to have a half-life of >1 day (33).

Similarly, van den Pol et al. reported that upon i.n. VSV infection, IFN-β, as well as IFN-λ2/3, expression was triggered within the olfactory bulb but not in the cerebellum and medulla. In contrast, ISG induction was detected in all brain areas tested (12). However, enhanced 2′,5′-oligoadenylate synthetase (OAS) induction was detected only in the olfactory bulb and not in other brain areas. This points toward particularly enhanced OAS triggering within the olfactory bulb. Such an enhanced IFNAR signaling within the olfactory bulb might also explain why we detected P-STAT-1 only in the granular layer of the olfactory bulb and not in distal brain areas. The observation that ISRE-eGFP mice devoid of IFN-β did not show enhanced eGFP expression upon i.n. VSV challenge (Fig. 3C, right panels) is explained by the absence of the dominating type I IFN of the CNS, i.e., IFN-β. In addition, it is possible that due to the absence of IFN-β priming, no low-level IFN-α responses could be induced any more.

In line with previous studies analyzing various different kinds of viruses, systemic induction of IFN-α was not altered in IFN-β$^{-/-}$ mice. In infection studies, their phenotype was less severe than that of IFNAR$^{-/-}$ mice. This suggested that, in addition to IFN-β, other type I IFN subtypes can take over regulatory functions *in vivo* (34).

The data discussed thus far imply that within the CNS, IFN-β induction plays a key role in limiting virus spread. We found here that upon i.n. VSV infection, locally induced IFN-β expressed primarily by astrocytes protects the entire brain. The biological relevance of this phenomenon was illustrated by the significantly enhanced sensitivity of IFN-β$^{-/-}$ mice to i.n. VSV infection, whereas such mice were as resistant to i.v. infection as WT controls. Thus, localized IFN expression within the olfactory bulb resulted in IFNAR triggering of distal parts of the CNS and mediated protection against VSV infection. Although the biological importance of the apparent redundancy of type I IFNs remains unclear, we demonstrated here the CNS-specific essential role of IFN-β in VSV infection.

ACKNOWLEDGMENTS

REFERENCES

1. **Sorgeloos F, Kreit M, Hermant P, Lardinois C, Michiels T.** 2013. Antiviral type I and type III interferon responses in the central nervous system. Viruses **5**:834–857. http://dx.doi.org/10.3390/v5030834.

2. **Griffin DE.** 2003. Immune responses to RNA-virus infections of the CNS. Nat Rev Immunol **3**:493–502. http://dx.doi.org/10.1038/nri1105.

3. **Dietzschold B, Rupprecht CE, Fu ZF, Koprowski H, Fields BN, Knipe DM, Howley PM.** 1996. Rhabdoviruses, p 1137–1159. *In* **Virology.** Lippincott-Raven Publishers, Philadelphia, PA.

4. **Detje CN, Meyer T, Schmidt H, Kreuz D, Rose JK, Bechmann I, Prinz M, Kalinke U.** 2009. Local type I IFN receptor signaling protects against virus spread within the central nervous system. J Immunol **182**:2297–2304. http://dx.doi.org/10.4049/jimmunol.0800596.

5. **Bi Z, Barna M, Komatsu T, Reiss CS.** 1995. Vesicular stomatitis virus infection of the central nervous system activates both innate and acquired immunity. J Virol **69**:6466–6472.

6. **Barchet W, Cella M, Odermatt B, Asselin-Paturel C, Colonna M, Kalinke U.** 2002. Virus-induced interferon alpha production by a dendritic cell subset in the absence of feedback signaling in vivo. J Exp Med **195**:507–516. http://dx.doi.org/10.1084/jem.20011666.

7. **Asselin-Paturel C, Boonstra A, Dalod M, Durand I, Yessaad N, Dezutter-Dambuyant C, Vicari A, O'Garra A, Biron C, Briere F, Trinchieri G.** 2001. Mouse type I IFN-producing cells are immature APCs with plasmacytoid morphology. Nat Immunol **2**:1144–1150. http://dx.doi.org/10.1038/ni736.

8. **Greter M, Heppner FL, Lemos MP, Odermatt BM, Goebels N, Laufer T, Noelle RJ, Becher B.** 2005. Dendritic cells permit immune invasion of the CNS in an animal model of multiple sclerosis. Nat Med **11**:328–334. http://dx.doi.org/10.1038/nm1197.

9. **Kallfass C, Ackerman A, Lienenklaus S, Weiss S, Heimrich B, Staeheli P.** 2012. Visualizing production of beta interferon by astrocytes and microglia in brain of La Crosse virus-infected mice. J Virol **86**:11223–11230. http://dx.doi.org/10.1128/JVI.01093-12.

10. **Kallfass C, Lienenklaus S, Weiss S, Staeheli P.** 2013. Visualizing the beta interferon response in mice during infection with influenza A viruses expressing or lacking nonstructural protein 1. J Virol **87**:6925–6930. http://dx.doi.org/10.1128/JVI.00283-13.

11. **Delhaye S, Paul S, Blakqori G, Minet M, Weber F, Staeheli P, Michiels T.** 2006. Neurons produce type I interferon during viral encephalitis. Proc Natl Acad Sci U S A **103**:7835–7840. http://dx.doi.org/10.1073/pnas.0602460103.

12. **van den Pol AN, Ding S, Robek MD.** 2014. Long-distance interferon signaling within the brain blocks virus spread. J Virol **88**:3695–3704. http://dx.doi.org/10.1128/JVI.03509-13.

13. **Akwa Y, Hassett DE, Eloranta ML, Sandberg K, Masliah E, Powell H, Whitton JL, Bloom FE, Campbell IL.** 1998. Transgenic expression of IFN-alpha in the central nervous system of mice protects against lethal neurotropic viral infection but induces inflammation and neurodegeneration. J Immunol **161**:5016–5026.

14. **Sandberg K, Eloranta ML, Campbell IL.** 1994. Expression of alpha/beta interferons (IFN-alpha/beta) and their relationship to IFN-alpha/beta-induced genes in lymphocytic choriomeningitis. J Virol **68**:7358–7366.

15. **Erlandsson L, Blumenthal R, Eloranta ML, Engel H, Alm G, Weiss S, Leanderson T.** 1998. Interferon-beta is required for interferon-alpha production in mouse fibroblasts. Curr Biol **8**:223–226. http://dx.doi.org/10.1016/S0960-9822(98)70086-7.

16. **Lienenklaus S, Cornitescu M, Zietara N, Lyszkiewicz M, Gekara N, Jablonska J, Edenhofer F, Rajewsky K, Bruder D, Hafner M, Staeheli P, Weiss S.** 2009. Novel reporter mouse reveals constitutive and inflammatory expression of IFN-beta in vivo. J Immunol **183**:3229–3236. http://dx.doi.org/10.4049/jimmunol.0804277.

17. **Tovey MG, Lallemand C, Meritet JF, Maury C.** 2006. Adjuvant activity of alpha interferon: mechanism(s) of action. Vaccine **24**(Suppl 2):S42–S47.

18. **Solodova E, Jablonska J, Weiss S, Lienenklaus S.** 2011. Production of IFN-beta during *Listeria monocytogenes* infection is restricted to monocyte/macrophage lineage. PLoS One **6**:e18543. http://dx.doi.org/10.1371/journal.pone.0018543.

19. **Tronche F, Kellendonk C, Kretz O, Gass P, Anlag K, Orban PC, Bock R, Klein R, Schutz G.** 1999. Disruption of the glucocorticoid receptor gene in the nervous system results in reduced anxiety. Nat Genet **23**:99–103. http://dx.doi.org/10.1038/12703.

20. **Zhu Y, Romero MI, Ghosh P, Ye Z, Charnay P, Rushing EJ, Marth JD, Parada LF.** 2001. Ablation of NF1 function in neurons induces abnormal development of cerebral cortex and reactive gliosis in the brain. Genes Dev **15**:859–876. http://dx.doi.org/10.1101/gad.862101.

21. **Bajenaru ML, Zhu Y, Hedrick NM, Donahoe J, Parada LF, Gutmann DH.** 2002. Astrocyte-specific inactivation of the neurofibromatosis 1 gene (NF1) is insufficient for astrocytoma formation. Mol Cell Biol **22**:5100–5113. http://dx.doi.org/10.1128/MCB.22.14.5100-5113.2002.

22. **Hövelmeyer N, Hao Z, Kranidioti K, Kassiotis G, Buch T, Frommer F, von Hoch L, Kramer D, Minichiello L, Kollias G, Lassmann H, Waisman A.** 2005. Apoptosis of oligodendrocytes via Fas and TNF-R1 is a key event in the

induction of experimental autoimmune encephalomyelitis. J Immunol 175:5875–5884. http://dx.doi.org/10.4049/jimmunol.175.9.5875.

23. Kotsiari A, Voss EV, Pul R, Skripuletz T, Ragancokova D, Trebst C, Stangel M. 2010. Interferon-beta treatment normalizes the inhibitory effect of serum from multiple sclerosis patients on oligodendrocyte progenitor proliferation. Neurosci Lett 485:107–111. http://dx.doi.org/10.1016/j.neulet.2010.08.075.

24. Hothorn T, Bretz F, Westfall P. 2008. Simultaneous inference in general parametric models. Biometrical J 50:346–363. http://dx.doi.org/10.1002/bimj.200810425.

25. Honda K, Yanai H, Takaoka A, Taniguchi T. 2005. Regulation of the type I IFN induction: a current view. Int Immunol 17:1367–1378. http://dx.doi.org/10.1093/intimm/dxh318.

26. Malmgaard L. 2004. Induction and regulation of IFNs during viral infections. J Interferon Cytokine Res 24:439–454. http://dx.doi.org/10.1089/1079990041689665.

27. Marie I, Durbin JE, Levy DE. 1998. Differential viral induction of distinct interferon-alpha genes by positive feedback through interferon regulatory factor-7. EMBO J 17:6660–6669. http://dx.doi.org/10.1093/emboj/17.22.6660.

28. Burdeinick-Kerr R, Wind J, Griffin DE. 2007. Synergistic roles of antibody and interferon in noncytolytic clearance of Sindbis virus from different regions of the central nervous system. J Virol 81:5628–5636. http://dx.doi.org/10.1128/JVI.01152-06.

29. Gerlach N, Schimmer S, Weiss S, Kalinke U, Dittmer U. 2006. Effects of type I interferons on Friend retrovirus infection. J Virol 80:3438–3444. http://dx.doi.org/10.1128/JVI.80.7.3438-3444.2006.

30. Trottier MD, Lyles DS, Reiss CS. 2007. Peripheral, but not central nervous system, type I interferon expression in mice in response to intranasal vesicular stomatitis virus infection. J Neurovirol 13:433–445. http://dx.doi.org/10.1080/13550280701460565.

31. Bush TG, Puvanachandra N, Horner CH, Polito A, Ostenfeld T, Svendsen CN, Mucke L, Johnson MH, Sofroniew MV. 1999. Leukocyte infiltration, neuronal degeneration, and neurite outgrowth after ablation of scar-forming, reactive astrocytes in adult transgenic mice. Neuron 23:297–308. http://dx.doi.org/10.1016/S0896-6273(00)80781-3.

32. Kasowski HJ, Kim H, Greer CA. 1999. Compartmental organization of the olfactory bulb glomerulus. J Comp Neurol 407:261–274. http://dx.doi.org/10.1002/(SICI)1096-9861(19990503)407:2<261::AID-CNE7>3.3.CO;2-7.

33. Andersen JB, Sternberg C, Poulsen LK, Bjorn SP, Givskov M, Molin S. 1998. New unstable variants of green fluorescent protein for studies of transient gene expression in bacteria. Appl Environ Microbiol 64:2240–2246.

34. Lazear HM, Pinto AK, Vogt MR, Gale M, Jr, Diamond MS. 2011. Beta interferon controls West Nile virus infection and pathogenesis in mice. J Virol 85:7186–7194. http://dx.doi.org/10.1128/JVI.00396-11.